Supplementary Materials

Large Ferroelectricity in $Hf_{0.85}Ce_{0.15}O_{2-\delta}$ Polycrystalline Thin Films via Lattice Expansion

Hangren Li[#, 1]; Jie Tu[#, 1]; Guoqiang Xi[#, 1]; Xiuqiao Liu[1]; Xudong Liu[1]; Siyuan Du[1]; Dongfei Lu[1]; Da Zu[2]; Yuxuan Zhang[3]; Qingxiao Wang[4]; Dongxing Zheng[5]; Xixiang Zhang[5]; Jianjun Tian[1]; Linxing Zhang[1, *]

1. Institute for Advanced Materials Technology, University of Science and Technology Beijing, Beijing 100083, China

2. Key Laboratory of Low Dimensional Materials and Application Technology of Ministry of Education, School of Materials Science and Engineering, Xiangtan University, Hunan 411105, China

3. School of Material and Metallurgy, Inner Mongolia University of Science and Technology, Baotou 014010, China.

4. Corelab, King Abdullah University of Science and Technology (KAUST), Thuwal 23955-6900, Saudi Arabia.

5. Physical Science and Engineering Division, King Abdullah University of Science and Technology (KAUST), Thuwal 23955-6900, Saudi Arabia.

# These authors contributed equally to this work.

SUPPLEMENTARY NOTES

1. Preparation of other thin films

To prepare the precursor, the required amount of cerium nitrate hexahydrate ($Ce(NO_3)_3$-$6H_2O$, Aladdin, 99.95%) and hafnium 2, 4-glutarate ($C_{20}H_{28}HfO_8$, Kindo, 97%) is dissolved in acetic acid, then 2, 4-pentanedione is added. A solution with a metal ion concentration of 0.1 mol/L is obtained, in which the ratio of acetic acid to 2, 4-pentanedione is 3:2. Finally, the mixed solvent was heated on a hot table at 75 °C for 2h to obtain a transparent precursor solution. In the preparation of Hf-Ce-O solid solution thin films, the precursor solution is spin coated on a 10×10 mm^2 $Si/SiO_2/Ti/Pt$ substrate and rotated at a high speed of 3500 rpm for 30 s. On the hot table, the water in the film was removed by heating at 120 °C for 3 min, and the organic solvent was removed by heating at 300 °C for 3 min. Once every 3 layers (total of 9 layers) for coating annealing treatment, then, using the hostler furnace respectively for $Hf_{(1-x)}Ce_xO_{2-\delta}$ (x = 0.6/0.9/0.12/0.15/0.18/0.21) under the 825 °C annealing, the annealing time about 20 min.

2. Effect of Pt electrode

XRD, XPS, STEM, and Raman measurements were tested without the presence of Pt electrode. The interfacial strain of the electrode can also affect the phase structure of HfO_2-based thin films [1]. However, the Pt electrode has the smaller surface tension than other common electrodes [2, 3]. In addition, the *P-E* loops of $Hf_{0.85}Ce_{0.15}O_{2-\delta}$ thin films with different thickness (Figure S4) suggest that the surface energy effect at the bottom interface (film/substrate) is not the key factor in O phase stability for the Ce substituted HfO_2 system. All the samples in this paper were tested for ferroelectric properties using Pt electrode, which indicates that the high remanent polarization of the T4 samples is indeed due to the stabilization of the O phase by the introduction of Ce elements and the dipole distortion caused by lattice expansion. Therefore, the interfacial strain introduced by the Pt electrode is not considered to be the key factor for the improvement of properties of $Hf_{0.85}Ce_{0.15}O_{2-\delta}$ thin films.

3. Impact of volume on the remanent polarization of HfO_2

In ferroelectrics, spontaneous polarization comes from the non-coincidence of positive and negative charge centers, so the value of spontaneous polarization is the sum of the product of charge (valence) and static displacement of each ion. However, in real crystals, the charge of the ion is often not the same as the valence, as the distribution of electron clouds of the same element in different crystals can vary. In order to accurately evaluate the charge of each HfO_2 ion, the processing method of Born effective charge is introduced, that is, the partial derivative of the electric dipole moment with respect to ion displacement is solved in the calculation, and the Born effective charge (Z*) is obtained. The results of the calculations are shown in Table S1-S15. The spontaneous polarization of HfO_2 crystals can be estimated by the formula (1-1) if the variation of polarization with ion displacement is approximated as a linear process.

$$P = \frac{e}{V}\sum_{i=1}^{m} Z_i^* \Delta u_i \qquad (1 - 1)$$

P - Spontaneous polarization of ferroelectrics (C/m^2)

e - Unit charge number (1.6×10^{-19} C)

V - Unit cell volume (m^3)

$\boldsymbol{Z}_i^*$ - Born effective charge on the i-th atom

$\boldsymbol{\Delta u_i}$ - Ferroelectric shift of the i-th atom (m)

In this paper, we calculate the spontaneous polarization strength of HfO_2 using the *P*bca phase as a reference phase. The crystal structure of the ferroelectric *P*ca2_1 phase has a point group of *I*mm_2 and is asymmetric only along the z-axis, while the x-axis and y-axis are symmetric, so that changes in the x-axis and y-axis have little effect on the ferroelectric polarization value.

4. Role of Ce element

Consider equation (1-1), The main factors affecting the macroscopic ferroelectric polarization of ferroelectric thin films are the unit cell volume and the Born effective charge of the system. We choose Ce elements with high Born effective charges to stabilize the orthorhombic phase [4]. In addition, the relative ratios of oxygen vacancy

(O_V) and lattice oxygen (O_L) as well as Ce^{3+} and Ce^{4+} in the HfO_2-based films can be effectively controlled by temperature to further control unit-cell volume [5]. Therefore, the introduction of the Ce element provides the dual effect of stabilizing the O-phase and the lattice expansion. Most reports still attribute improvements in ferroelectricity only to the size effects, crystallinity, and stability of the orthorhombic phase [6, 7], both experimental and theoretical studies. Our work provides a new way to break through the performance barrier of hafnium-based polycrystalline thin films.

5. DFT calculation

5.1 Phase stability calculation model

The calculations were carried out by building a $1 \times 1 \times 1$ unit cell using the Castep-selected fictitious crystal approximation (*Mterials Studio 2019*), with Ce concentrations of 0/3/6/9/12/15/18/21 % in the C/O/T/M phase, respectively. The electron exchange-correlation interactions were explained by the Generalised Gradient Approximation (GGA) [8], the electron exchange dependent interaction is explained by Perdew-Burke-Ernzerhof (PBE). The plane wave basis cut-off energy was determined to be 550 eV through convergence testing. A 3 × 3 × 3 Monkhorst-Pack k-point grid was used. The energy is $1.0 \times e^{-5}$, with a maximum force of 0.03 eV/Å, a maximum stress of 0.05 GPa, and a maximum displacement of 0.001 Å.

5.2 Born effective charge calculation of ferroelectric polarization

The specific values of Born effective charge are obtained by running in the Castep-selected fictitious crystal approximation (*Mterials Studio 2019*). The electron exchange-correlation interactions were explained by the GGA [8], the electron exchange dependent interaction is explained by PBE. A 3 × 3 × 3 Monkhorst-Pack k-point grid was used. The convergence criterion for the energy change, maximum force, maximum stress, and maximum displacement was set to 750 eV, 10^{-5} eV/atom, 0.03 eV/ Å, 0.05 GPa, and 10^{-3} Å.

SUPPLEMENTARY FIGURES

1. DFT calculations of the effect of different concentrations of Ce-sites on the stability of the hafnium oxide phase.

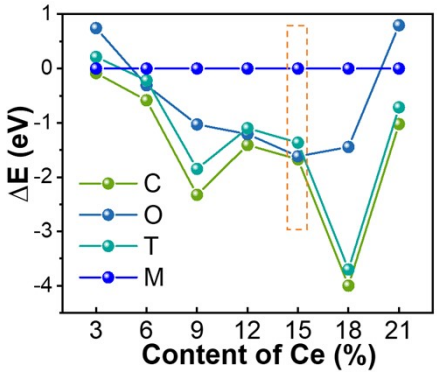

Figure S1. DFT calculations were conducted to determine the phase stability of $Hf_{(1-x)}Ce_xO_{2-\delta}$ with varying Ce concentrations (x = 0/0.03/0.06/0.09/0.12/0.15/0.18/0.21).

The stability of the C/O/T phase compared to the M phase following Ce doping in HfO_2 was calculated using DFT. To investigate the stability of the doped HfO_2, we analyzed the change in relative energy ΔE_r for each phase. The calculation method used is defined (1-2). According to the calculations in Figure S1, the O phase is expected to exhibit higher stability at Ce = 15 %. Furthermore, this is consistent with the findings obtained from XRD and electric hysteresis loop measurements. Where, $E_{\xi(\text{doped})}$ and $E_{\xi(\text{pure})}$ represent the total energy of C/O/T phase with and without impurities, respectively.

$$\Delta E_r = \frac{E_{\xi(\text{doped})} - E_{m(\text{doped})}}{E_{\xi(\text{pure})} - E_{m(\text{pure})}} \quad (1-2)$$

2. Phase of $Hf_{1-x}Ce_xO_{2-\delta}$ (x = 0.6/0.9/0.12/0.15/0.18/0.21) thin films changes with varying Ce concentrations.

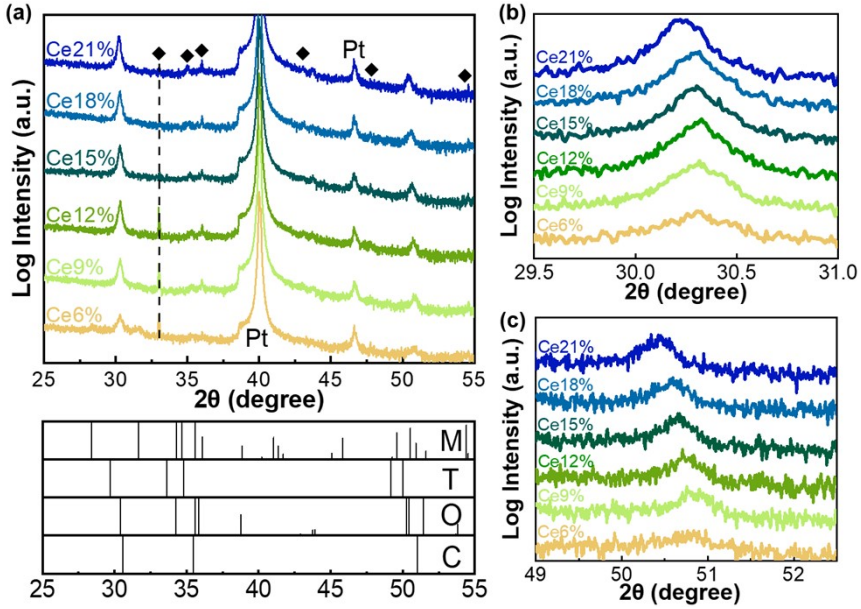

Figure S2. (a) XRD $Hf_{1-x}Ce_xO_{2-\delta}$ (x = 0.6/0.9/0.12/0.15/0.18/0.21). (b) and (c) XRD detail magnification.

XRD analysis reveals that the samples exhibit some M-phase content at the Ce concentration of 6 %. The characteristic peak of the M-phase disappears when the Ce content reaches 9 % or above. This suggests that the introduction of Ce has the potential to suppress M-phase production and encourage O-phase formation. Figures S2 (b) and (c) illustrate that with the increase in Ce content, there is a shift towards a smaller angle for $(111)_O$ and $(220)_O$. This phenomenon occurs because Ce atoms have a larger radius than Hf atoms, leading to an increase in the volume of the entire unit-cell of the thin films. It is important to note that we use "◆" to label diffraction peaks originating from the Pt/Ti/SiO_2/Si substrates. They come from the diffraction of the substrate with respect to X-rays of other wavelengths, such as the diffraction peak of Si (004) plane at ~ 33.19° from the Cu K_α X-ray diffraction with second harmonics (~ 0.77 Å), the diffraction peak of Pt (111) plane at ~ 36.19° from Cu K_β X-rays (~ 1.39 Å), the diffraction peak of Pt (200) plane at ~ 46.9° from Cu K_α X-rays (~ 1.54 Å), and the diffraction peak of Si (004) plane at ~ 54.7° from W $L_{\beta 2}$ X-rays (~ 1.24 Å). The peak of ~ 33.19° was sometimes absent, which might be due to the fact that vector superposition

of X-rays is difficult to occur in a common XRD diffractometer.

3. Typical *P-E* loops of $Hf_{1-x}Ce_xO_{2-\delta}$ (x = 0.6/0.9/0.12/0.15/0.18/0.21) thin films

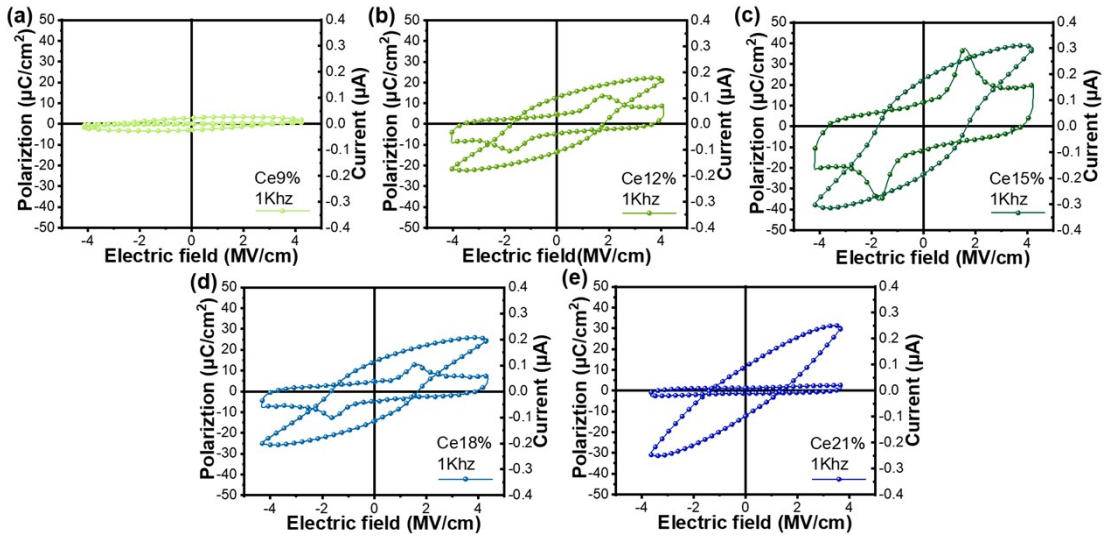

Figure S3. Ferroelectric polarization for $Hf_{1-x}Ce_xO_{2-\delta}$ (x = 0.6/0.9/0.12/0.15/0.18/0.21) thin films.

Figure S3. illustrates the trend of sample P_r value as a function of increasing Ce doping concentration, with Ce of 15 % exhibiting the highest P_r value.

4. Typical *P-E* loops of $Hf_{0.85}Ce_{0.15}O_{2-\delta}$ (different thicknesses) thin films

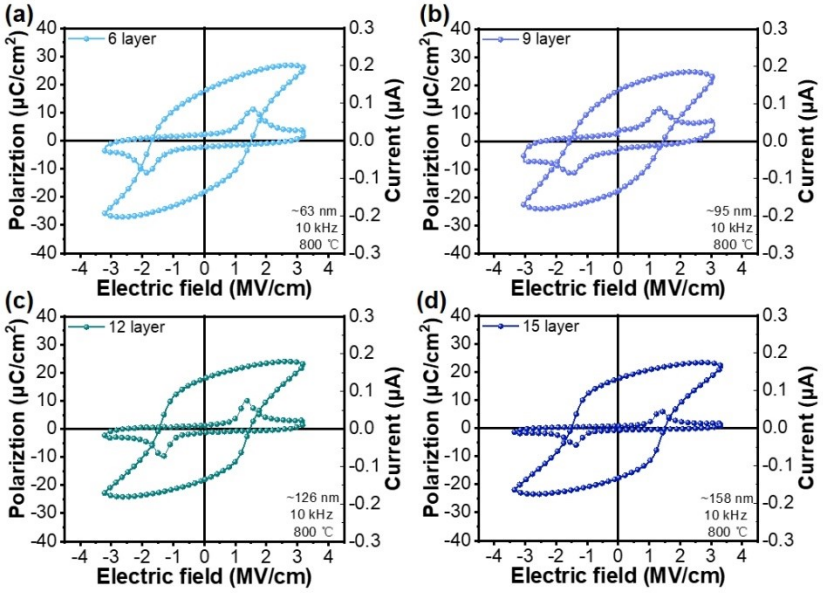

Figure S4. Ferroelectric properties of $Hf_{0.85}Ce_{0.15}O_{2-\delta}$ thin films with different layers. (a) 6 layers about 63 nm. (b) 9 layers about 95 nm. (c) 12 layers about 126 nm. (d) 15 layers about 158 nm. The layer means the spin-coating number in the preparation of the film.

Figure S4 shows the influence of P_r value of $Hf_{0.85}Ce_{0.15}O_{2-\delta}$ thin films with thickness. The ferroelectric remanent polarization value of $Hf_{0.85}Ce_{0.15}O_{2-\delta}$ thin films has no obvious dependence on thickness. This indicates the thickness with surface energy effect is not the key factor in O phase stability for present system. The reason of the remanent polarization enhancement is considered to be derived from the combined effect of the stabilization of the thin films O phase by the introduction of Ce elements and the increase of the dipole distortion.

5. Effect of temperature on ferroelectricity of $Hf_{0.85}Ce_{0.15}O_{2-\delta}$ thin films (T1-T5)

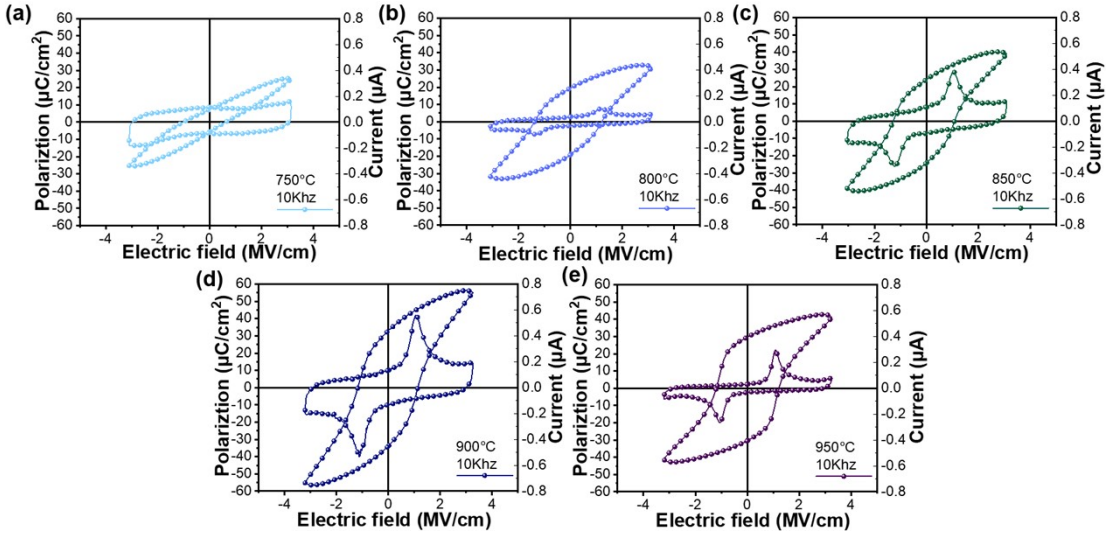

Figure S5. The ferroelectric properties of *P-E* loops of $Hf_{0.85}Ce_{0.15}O_{2-\delta}$ thin films at different temperatures were determined at room temperature.

6. Phase images of $Hf_{0.85}Ce_{0.15}O_{2-\delta}$ thin films (T1-T5) by PFM

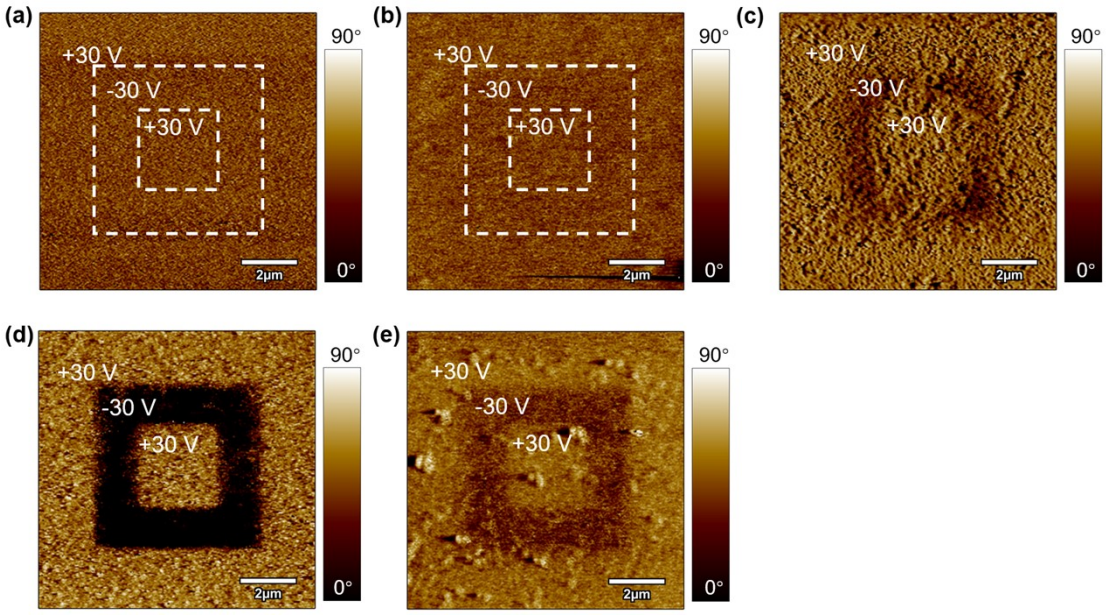

Figure S6. Phase images of $Hf_{0.85}Ce_{0.15}O_{2-\delta}$ thin films. (a) T1. (b) T2. (c) T3. (d) T4. (e) T5.

7. Amplitude information images of $Hf_{0.85}Ce_{0.15}O_{2-\delta}$ thin films (T1-T5) by PFM

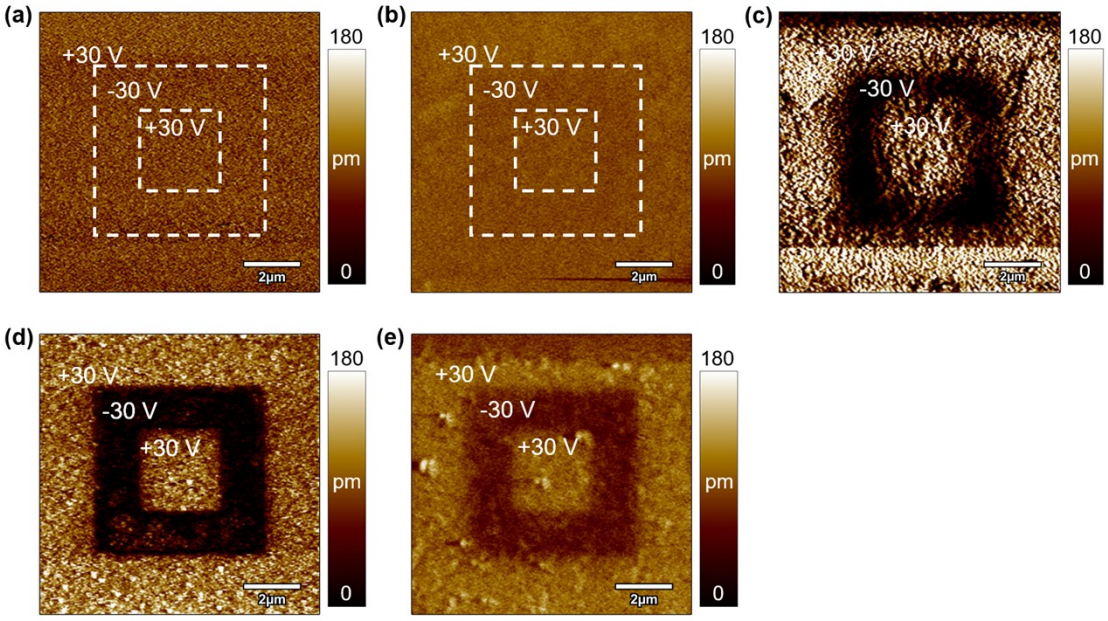

Figure S7. Amplitude images of $Hf_{0.85}Ce_{0.15}O_{2-\delta}$ thin films. (a) T1. (b) T2. (c) T3. (d) T4. (e) T5.

8. PUND triangle wave type applied on $Hf_{0.85}Ce_{0.15}O_{2-\delta}$ thin films (T4)

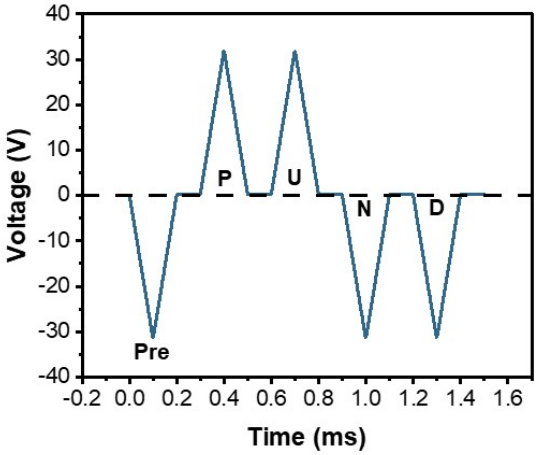

Figure S8. Time versus triangular wave voltage curve in PUND mode.

9. Ferroelectric fatigue and leakage current test

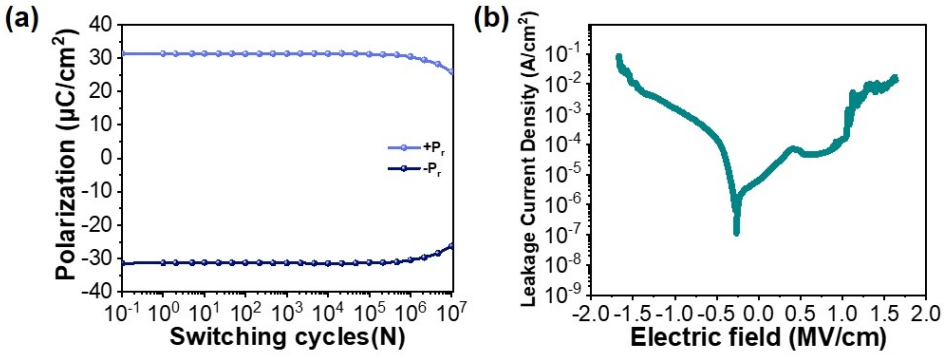

Figure S9. (a) Ferroelectric fatigue test of T4 samples. We applied fatigue using a fatigue frequency of 100 kHz and a fatigue electric field of about 2 MV/cm, which is closed to twice the coercive field. As in the test of the ferroelectric hysteresis loops in the text, we read the *P-E* loops using a frequency of 10 kHz and an electric field of about 3 MV/cm. (b) Leakage current test of T4 samples.

10. Morphology of $Hf_{0.85}Ce_{0.15}O_{2-\delta}$ thin films (T1-T5)

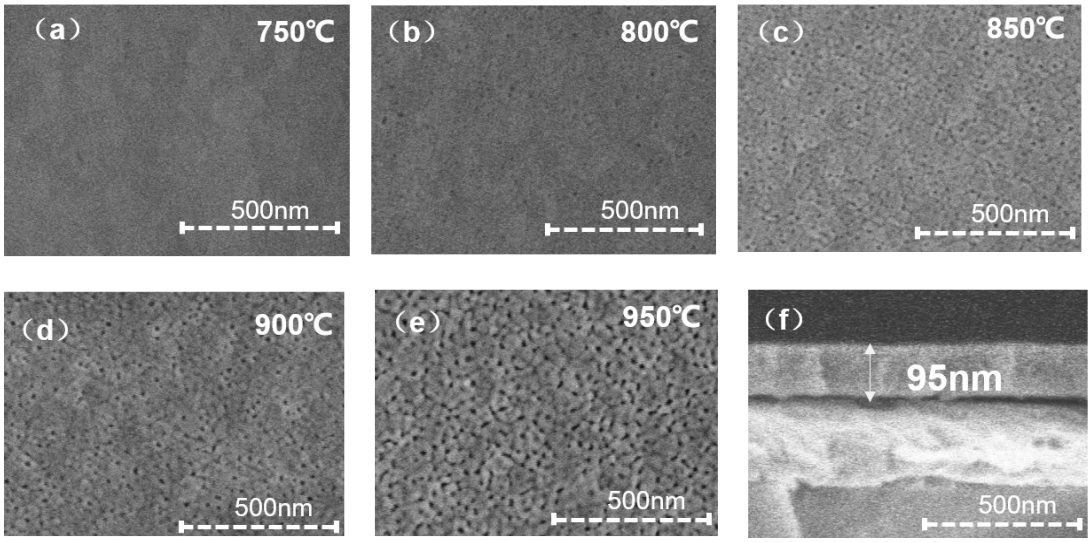

Figure S10. The SEM images for $Hf_{0.85}Ce_{0.15}O_{2-\delta}$ thin films. (a) T1. (b) T2. (c) T2. (d) T4. (e) T5. The sample's roughness increases gradually with temperature increase. With the increase of the preparation temperature, the number of pores on the ferroelectric thin films surface will increase (Figure S10d) [9]. This may cause the leakage current of the thin films to rise. The TEM cross-section analysis revealed there are some pores on the surface of the $Hf_{0.85}Ce_{0.15}O_{2-\delta}$ thin films while the pores inside the film are relative few (Figure 2d). In leakage current tests, T4 samples had small leakage that is only 10^{-7} A/cm^2 (Figure S9). This value also matches the leakage current reported (~ 10^{-7} A/cm^2) in the previous paper [10]. This indicates that there are fewer internal defects in the thin films. Although there are some surface pores, they will have little impact on the use of future devices.

11. TEM of $Hf_{0.85}Ce_{0.15}O_{2-\delta}$ thin films

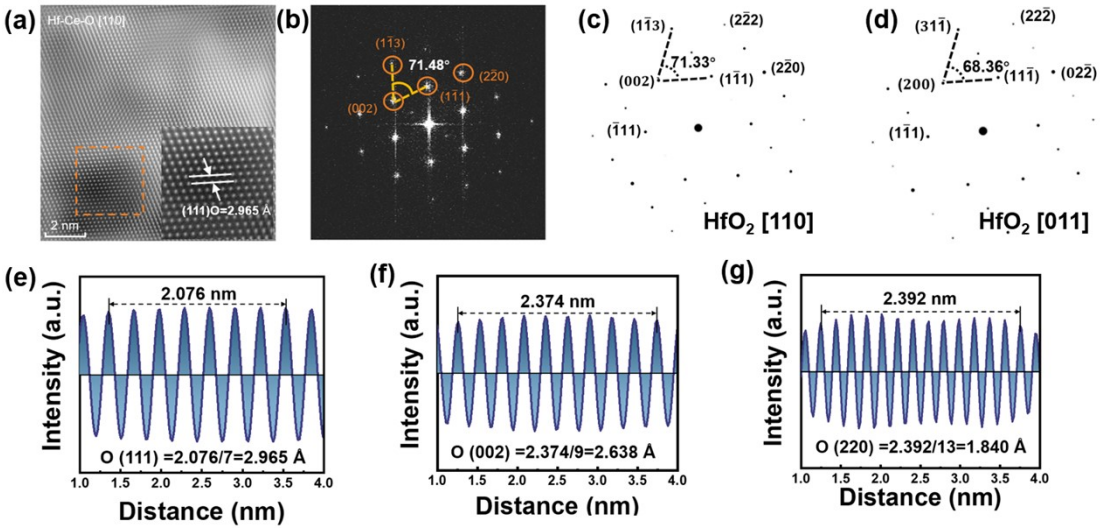

Figure S11. The O-phase crystal plane spacing was measured by TEM. (a) Atomic-scale HAADF-STEM images of $Hf_{0.85}Ce_{0.15}O_{2-\delta}$ thin films. (b) Corresponding FFT pattern of Figure S11 (a). (c) Standard FFT pattern of HfO_2 along the [110] direction by simulating. (d) Standard FFT pattern of HfO_2 along the [011] direction by simulating. (e, f, g) Interplanar spacing of O (111) (e), O (002) (f), and O (220) (g).

As shown in Fig. S11, the interplanar spacing of $(111)_O/(220)_O/(002)_O$ is 2.965 Å /1.840 Å/2638 Å, respectively. Since phase O [110] is similar to the diffraction spots of [011], it is impossible to determine which axial arrangement is based on the FFT arrangement. But we can find that in the standard HfO_2 diffraction spot in the [110] axial $(11\bar{3})$ - (002) - $(1\bar{1}1)$ angle is 71.33°, and in the [011] axial $(31\bar{1})$ - (200) - $(11\bar{1})$ angle is 68.36 °. In our chosen area $(11\bar{3})$ - (002) - $(1\bar{1}1)$ has an angle of 71.48°, so we consider the region to be [110] axial.

12. High resolution O1*s* and Ce 3*d* XPS spectra for $Hf_{0.85}Ce_{0.15}O_{2-\delta}$ thin films (T2, T3, and T5).

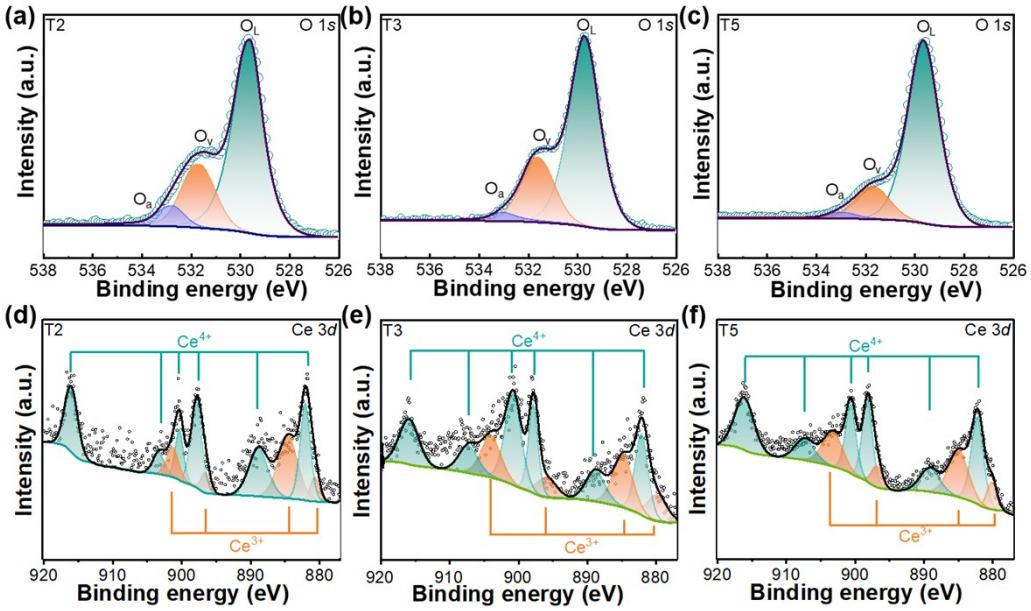

Figure S12. High resolution XPS spectra of (a) T2, (b) T3, and T5 O 1*s* XPS spectra for $Hf_{0.85}Ce_{0.15}O_{2-\delta}$ thin films. (d) T2, (e) T3, and (f) T5 Ce 3*d* XPS spectra for $Hf_{0.85}Ce_{0.15}O_{2-\delta}$ thin films.

Table S1. $Pca2_1$ of HfO_2 (a = 5.234 Å, b = 5.010 Å, c = 5.043 Å. P_r ~ 49.28 μC/cm^2)

Element	Born Effective Charges			
		x	***y***	***z***
O1	***x***	-2.31245	-0.65657	0.25144
	y	-0.80245	-2.92394	-0.7594
	z	0.1667	-0.8019	-2.62735
O2	***x***	-2.41452	-0.26913	0.10436
	y	-0.28531	-2.60219	0.46477
	z	0.11885	0.53252	-2.59385
O3	***x***	-2.31245	-0.6565	-0.2515
	y	-0.80243	-2.92387	0.75938
	z	-0.16676	0.80188	-2.62739
O4	***x***	-2.4145	-0.26914	-0.10436
	y	-0.28526	-2.60218	-0.46478
	z	-0.11883	-0.53252	-2.59386
O5	***x***	-2.31246	0.65653	0.25154
	y	0.8024	-2.92386	0.75933
	z	0.16681	0.80182	-2.62737
O6	***x***	-2.41455	0.26917	0.1044
	y	0.28533	-2.60221	-0.46478
	z	0.11885	-0.53254	-2.59388
O7	***x***	-2.31246	0.65655	-0.2515
	y	0.80248	-2.92392	-0.75936
	z	-0.1668	-0.80187	-2.62734
O8	***x***	-2.41449	0.26911	-0.10435
	y	0.28524	-2.60221	0.46481
	z	-0.11881	0.53258	-2.59386
Hf1	***x***	4.72698	-0.26028	-0.1434
	y	0.02895	5.52618	0.20101
	z	-0.06106	0.14643	5.22126
Hf2	***x***	4.72697	-0.26028	0.14338
	y	0.02895	5.5261	-0.20098
	z	0.06105	-0.14642	5.22123
Hf3	***x***	4.72696	0.26026	-0.14336
	y	-0.02894	5.52603	-0.20095
	z	-0.06101	-0.14638	5.22121
Hf4	***x***	4.72696	0.26028	0.14336
	y	-0.02896	5.52606	0.20094

	z	0.06102	0.14641	5.22122

Table S2. *P*ca2$_1$ of HfO_2 (*a* = 5.234 Å, *b* = 5.010 Å, *c* = 5.243 Å, P_r ~ 51.54 μC/cm^2)

Element	**Born Effective Charges**			
		x	***y***	***z***
O1	***x***	-2.41395	-0.8725	0.19909
	y	-0.9558	-2.86695	-0.79248
	z	-0.0003	-0.78693	-2.92619
O2	***x***	-2.41494	-0.8728	-0.19885
	y	-0.95574	-2.86617	0.79164
	z	0.00065	0.78612	-2.92539
O3	***x***	-2.41395	-0.8725	-0.19909
	y	-0.9558	-2.86695	0.79248
	z	0.0003	0.78693	-2.92619
O4	***x***	-2.41494	-0.8728	0.19885
	y	-0.95574	-2.86617	-0.79164
	z	-0.00065	-0.78612	-2.92539
O5	***x***	-2.41395	0.8725	0.19909
	y	0.9558	-2.86695	0.79248
	z	-0.0003	0.78693	-2.92619
O6	***x***	-2.41494	0.8728	-0.19885
	y	0.95574	-2.86617	-0.79164
	z	0.00065	-0.78612	-2.92539
O7	***x***	-2.41395	0.8725	-0.19909
	y	0.9558	-2.86695	-0.79248
	z	0.0003	-0.78693	-2.92619
O8	***x***	-2.41494	0.8728	0.19885
	y	0.95574	-2.86617	0.79164
	z	-0.00065	0.78612	-2.92539
Hf1	***x***	4.82889	-0.00048	-0.00047
	y	0.00023	5.73311	0.28556
	z	-0.00004	0.42668	5.85158
Hf2	***x***	4.82889	-0.00048	0.00047
	y	0.00023	5.73311	-0.28556
	z	0.00004	-0.42668	5.85158
Hf3	***x***	4.82889	0.00048	-0.00047
	y	-0.00023	5.73311	-0.28556
	z	-0.00004	-0.42668	5.85158
Hf4	***x***	4.82889	0.00048	0.00047

	y	-0.00023	5.73311	0.28556
	z	0.00004	0.42668	5.85158

Table S3. *P*ca2$_1$ of HfO_2 (*a* = 5.234 Å, *b* = 5.010 Å, *c* = 5.443 Å, P_r ~ 57.47 μC/cm^2)

Element	**Born Effective Charges**			
		x	***y***	***z***
O1	***x***	-2.45928	-0.95149	0.20905
	y	-1.05101	-2.80099	-0.72711
	z	0.00463	-0.73131	-3.00603
O2	***x***	-2.45773	-0.94976	-0.2092
	y	-1.04805	-2.79963	0.72702
	z	-0.00427	0.73073	-3.0088
O3	***x***	-2.45928	-0.95149	-0.20905
	y	-1.05101	-2.80099	0.72711
	z	-0.00463	0.73131	-3.00603
O4	***x***	-2.45773	-0.94976	0.2092
	y	-1.04805	-2.79963	-0.72702
	z	0.00427	-0.73073	-3.0088
O5	***x***	-2.45928	0.95149	0.20905
	y	1.05101	-2.80099	0.72711
	z	0.00463	0.73131	-3.00603
O6	***x***	-2.45773	0.94976	-0.2092
	y	1.04805	-2.79963	-0.72702
	z	-0.00427	-0.73073	-3.0088
O7	***x***	-2.45928	0.95149	-0.20905
	y	1.05101	-2.80099	-0.72711
	z	-0.00463	-0.73131	-3.00603
O8	***x***	-2.45773	0.94976	0.2092
	y	1.04805	-2.79963	0.72702
	z	0.00427	0.73073	-3.0088
Hf1	***x***	4.91702	-0.00369	-0.00424
	y	0.00205	5.60062	0.36147
	z	-0.00118	0.56205	6.01484
Hf2	***x***	4.91702	-0.00369	0.00424
	y	0.00205	5.60062	-0.36147
	z	0.00118	-0.56205	6.01484
Hf3	***x***	4.91702	0.00369	-0.00424
	y	-0.00205	5.60062	-0.36147
	z	-0.00118	-0.56205	6.01484

Hf4	***x***	4.91702	0.00369	0.00424
	y	-0.00205	5.60062	0.36147
	z	0.00118	0.56205	6.01484

Table S4. *P*ca2$_1$ of HfO_2 (a = 5.234 Å, b = 5.010 Å, c = 5.643 Å, P_r ~ 67.01 μC/cm^2)

Element	**Born Effective Charges**			
		x	***y***	***z***
O1	***x***	-2.5147	-0.99573	0.22472
	y	-1.1253	-2.71316	-0.6145
	z	0.01955	-0.62756	-3.03957
O2	***x***	-2.4797	-0.9648	-0.23043
	y	-1.08165	-2.70317	0.63889
	z	-0.01941	0.65537	-3.10112
O3	***x***	-2.5147	-0.99573	-0.22472
	y	-1.1253	-2.71316	0.6145
	z	-0.01955	0.62756	-3.03957
O4	***x***	-2.4797	-0.9648	0.23043
	y	-1.08165	-2.70317	-0.63889
	z	0.01941	-0.65537	-3.10112
O5	***x***	-2.5147	0.99573	0.22472
	y	1.1253	-2.71316	0.6145
	z	0.01955	0.62756	-3.03957
O6	***x***	-2.4797	0.9648	-0.23043
	y	1.08165	-2.70317	-0.63889
	z	-0.01941	-0.65537	-3.10112
O7	***x***	-2.5147	0.99573	-0.22472
	y	1.1253	-2.71316	-0.6145
	z	-0.01955	-0.62756	-3.03957
O8	***x***	-2.4797	0.9648	0.23043
	y	1.08165	-2.70317	0.63889
	z	0.01941	0.65537	-3.10112
Hf1	***x***	4.9944	-0.01895	-0.00607
	y	0.00065	5.41633	0.44407
	z	-0.00664	0.70873	6.14069
Hf2	***x***	4.9944	-0.01895	0.00607
	y	0.00065	5.41633	-0.44407
	z	0.00664	-0.70873	6.14069
Hf3	***x***	4.9944	0.01895	-0.00607
	y	-0.00065	5.41633	-0.44407

	z	-0.00664	-0.70873	6.14069
Hf4	***x***	4.9944	0.01895	0.00607
	y	-0.00065	5.41633	0.44407
	z	0.00664	0.70873	6.14069

Table S5. *P*ca2$_1$ of HfO_2 (*a* = 5.334 Å, *b* = 5.010 Å, *c* = 5.043 Å, P_r ~ 48.83 μC/cm^2)

Element	**Born Effective Charges**			
		x	***y***	***z***
O1	***x***	-2.39847	-0.81321	0.18195
	y	-0.86917	-2.88469	-0.82234
	z	-0.00356	-0.82383	-2.81847
O2	***x***	-2.39867	-0.81321	-0.18277
	y	-0.869	-2.88429	0.82319
	z	0.00319	0.82483	-2.8186
O3	***x***	-2.39847	-0.81321	-0.18195
	y	-0.86917	-2.88469	0.82234
	z	0.00356	0.82383	-2.81847
O4	***x***	-2.39867	-0.81321	0.18277
	y	-0.869	-2.88429	-0.82319
	z	-0.00319	-0.82483	-2.8186
O5	***x***	-2.39847	0.81321	0.18195
	y	0.86917	-2.88469	0.82234
	z	-0.00356	0.82383	-2.81847
O6	***x***	-2.39867	0.81321	-0.18277
	y	0.869	-2.88429	-0.82319
	z	0.00319	-0.82483	-2.8186
O7	***x***	-2.39847	0.81321	-0.18195
	y	0.86917	-2.88469	-0.82234
	z	0.00356	-0.82383	-2.81847
O8	***x***	-2.39867	0.81321	0.18277
	y	0.869	-2.88429	0.82319
	z	-0.00319	0.82483	-2.8186
Hf1	***x***	4.79714	0.00085	0.00094
	y	0.00037	5.76898	0.23128
	z	0.00031	0.27844	5.63708
Hf2	***x***	4.79714	0.00085	-0.00094
	y	0.00037	5.76898	-0.23128
	z	-0.00031	-0.27844	5.63708
Hf3	***x***	4.79714	-0.00085	0.00094

	y	-0.00037	5.76898	-0.23128
	z	0.00031	-0.27844	5.63708
Hf4	***x***	4.79714	-0.00085	-0.00094
	y	-0.00037	5.76898	0.23128
	z	-0.00031	0.27844	5.63708

Table S6. *P*ca2$_1$ of HfO_2 (*a* = 5.434 Å, *b* = 5.010 Å, *c* = 5.043 Å, P_r ~ 47.93 μC/cm^2)

Element	**Born Effective Charges**			
		x	***y***	***z***
O1	***x***	-2.43275	-0.88597	0.18613
	y	-0.93094	-2.87779	-0.82657
	z	-0.0152	-0.83362	-2.80523
O2	***x***	-2.43062	-0.87752	-0.18354
	y	-0.91922	-2.87416	0.8292
	z	0.01576	0.8365	-2.81087
O3	***x***	-2.43275	-0.88597	-0.18613
	y	-0.93094	-2.87779	0.82657
	z	0.0152	0.83362	-2.80523
O4	***x***	-2.43062	-0.87752	0.18354
	y	-0.91922	-2.87416	-0.8292
	z	-0.01576	-0.8365	-2.81087
O5	***x***	-2.43275	0.88597	0.18613
	y	0.93094	-2.87779	0.82657
	z	-0.0152	0.83362	-2.80523
O6	***x***	-2.43062	0.87752	-0.18354
	y	0.91922	-2.87416	-0.8292
	z	0.01576	-0.8365	-2.81087
O7	***x***	-2.43275	0.88597	-0.18613
	y	0.93094	-2.87779	-0.82657
	z	0.0152	-0.83362	-2.80523
O8	***x***	-2.43062	0.87752	0.18354
	y	0.91922	-2.87416	0.8292
	z	-0.01576	0.8365	-2.81087
Hf1	***x***	4.86338	-0.0067	-0.00979
	y	0.00399	5.75195	0.22916
	z	-0.00436	0.26061	5.6161
Hf2	***x***	4.86338	-0.0067	0.00979
	y	0.00399	5.75195	-0.22916
	z	0.00436	-0.26061	5.6161

Hf3	***x***	4.86338	0.0067	-0.00979
	y	-0.00399	5.75195	-0.22916
	z	-0.00436	-0.26061	5.6161
Hf4	***x***	4.86338	0.0067	0.00979
	y	-0.00399	5.75195	0.22916
	z	0.00436	0.26061	5.6161

Table S7. *P*ca2$_1$ of HfO_2 (*a* = 5.534 Å, *b* = 5.010 Å, *c* = 5.043 Å, P_r ~ 47.10 μC/cm^2)

Element	**Born Effective Charges**			
		x	***y***	***z***
O1	***x***	-2.45396	-0.916	0.17932
	y	-0.9476	-2.85824	-0.83401
	z	-0.02481	-0.84622	-2.79825
O2	***x***	-2.45614	-0.91736	-0.18003
	y	-0.94849	-2.85817	0.83188
	z	0.02445	0.84461	-2.7983
O3	***x***	-2.45396	-0.916	-0.17932
	y	-0.9476	-2.85824	0.83401
	z	0.02481	0.84622	-2.79825
O4	***x***	-2.45614	-0.91736	0.18003
	y	-0.94849	-2.85817	-0.83188
	z	-0.02445	-0.84461	-2.7983
O5	***x***	-2.45396	0.916	0.17932
	y	0.9476	-2.85824	0.83401
	z	-0.02481	0.84622	-2.79825
O6	***x***	-2.45614	0.91736	-0.18003
	y	0.94849	-2.85817	-0.83188
	z	0.02445	-0.84461	-2.7983
O7	***x***	-2.45396	0.916	-0.17932
	y	0.9476	-2.85824	-0.83401
	z	0.02481	-0.84622	-2.79825
O8	***x***	-2.45614	0.91736	0.18003
	y	0.94849	-2.85817	0.83188
	z	-0.02445	0.84461	-2.7983
Hf1	***x***	4.91009	0.00062	0.00109
	y	0.00054	5.71641	0.21424
	z	0.00051	0.23374	5.59654
Hf2	***x***	4.91009	0.00062	-0.00109
	y	0.00054	5.71641	-0.21424

	z	-0.00051	-0.23374	5.59654
Hf3	***x***	4.91009	-0.00062	0.00109
	y	-0.00054	5.71641	-0.21424
	z	0.00051	-0.23374	5.59654
Hf4	***x***	4.91009	-0.00062	-0.00109
	y	-0.00054	5.71641	0.21424
	z	-0.00051	0.23374	5.59654

Table S8. *P*ca2$_1$ of HfO_2 (a = 5.634 Å, b = 5.010 Å, c = 5.043 Å, P_r ~ 47.09 μC/cm^2)

Element	**Born Effective Charges**			
		x	***Y***	***z***
O1	***x***	-2.4646	-0.93657	0.17107
	y	-0.95042	-2.84157	-0.84386
	z	-0.0328	-0.8631	-2.78826
O2	***x***	-2.46668	-0.94097	-0.16821
	y	-0.95899	-2.84409	0.84358
	z	0.03652	0.86156	-2.78417
O3	***x***	-2.4646	-0.93657	-0.17107
	y	-0.95042	-2.84157	0.84386
	z	0.0328	0.8631	-2.78826
O4	***x***	-2.46668	-0.94097	0.16821
	y	-0.95899	-2.84409	-0.84358
	z	-0.03652	-0.86156	-2.78417
O5	***x***	-2.4646	0.93657	0.17107
	y	0.95042	-2.84157	0.84386
	z	-0.0328	0.8631	-2.78826
O6	***x***	-2.46668	0.94097	-0.16821
	y	0.95899	-2.84409	-0.84358
	z	0.03652	-0.86156	-2.78417
O7	***x***	-2.4646	0.93657	-0.17107
	y	0.95042	-2.84157	-0.84386
	z	0.0328	-0.8631	-2.78826
O8	***x***	-2.46668	0.94097	0.16821
	y	0.95899	-2.84409	0.84358
	z	-0.03652	0.86156	-2.78417
Hf1	***x***	4.93129	0.00131	0.00335
	y	-0.00573	5.68566	0.19757
	z	0.00237	0.19964	5.57243
Hf2	***x***	4.93129	0.00131	-0.00335
	y	-0.00573	5.68566	-0.19757

	z	-0.00237	-0.19964	5.57243
Hf3	***x***	4.93129	-0.00131	0.00335
	y	0.00573	5.68566	-0.19757
	z	0.00237	-0.19964	5.57243
Hf4	***x***	4.93129	-0.00131	-0.00335
	y	0.00573	5.68566	0.19757
	z	-0.00237	0.19964	5.57243

Table S9. $Pca2_1$ of HfO_2 (a = 5.834 Å, b = 5.010 Å, c = 5.043 Å, $P_r \sim 45.27$ μC/cm^2)

Element	**Born Effective Charges**			
		x	***Y***	***z***
O1	***x***	-2.45931	-0.97383	0.14438
	y	-0.95399	-2.81628	-0.87227
	z	-0.05706	-0.90549	-2.76457
O2	***x***	-2.45139	-0.96924	-0.14016
	y	-0.9527	-2.81873	0.88066
	z	0.06007	0.91114	-2.76827
O3	***x***	-2.45931	-0.97383	-0.14438
	y	-0.95399	-2.81628	0.87227
	z	0.05706	0.90549	-2.76457
O4	***x***	-2.45139	-0.96924	0.14016
	y	-0.9527	-2.81873	-0.88066
	z	-0.06007	-0.91114	-2.76827
O5	***x***	-2.45931	0.97383	0.14438
	y	0.95399	-2.81628	0.87227
	z	-0.05706	0.90549	-2.76457
O6	***x***	-2.45139	0.96924	-0.14016
	y	0.9527	-2.81873	-0.88066
	z	0.06007	-0.91114	-2.76827
O7	***x***	-2.45931	0.97383	-0.14438
	y	0.95399	-2.81628	-0.87227
	z	0.05706	-0.90549	-2.76457
O8	***x***	-2.45139	0.96924	0.14016
	y	0.9527	-2.81873	0.88066
	z	-0.06007	0.91114	-2.76827
Hf1	***x***	4.9107	-0.00254	-0.00385
	y	-0.00445	5.63502	0.1668
	z	-0.00154	0.12219	5.53284
Hf2	***x***	4.9107	-0.00254	0.00385
	y	-0.00445	5.63502	-0.1668
	z	0.00154	-0.12219	5.53284

Hf3	***x***	4.9107	0.00254	-0.00385
	y	0.00445	5.63502	-0.1668
	z	-0.00154	-0.12219	5.53284
Hf4	***x***	4.9107	0.00254	0.00385
	y	0.00445	5.63502	0.1668
	z	0.00154	0.12219	5.53284

Table S10. *P*ca2$_1$ of HfO_2 (*a* = 5.234 Å, *b* = 5.110 Å, *c* = 5.043 Å, $P_r \sim 48.25$ μC/cm^2)

Element	**Born Effective Charges**			
		x	***Y***	***z***
O1	***x***	-2.34869	-0.75865	0.19839
	y	-0.83928	-2.9426	-0.81367
	z	0.0094	-0.8111	-2.81128
O2	***x***	-2.3476	-0.75978	-0.19985
	y	-0.84091	-2.94359	0.8145
	z	-0.01052	0.81165	-2.81025
O3	***x***	-2.34869	-0.75865	-0.19839
	y	-0.83928	-2.9426	0.81367
	z	-0.0094	0.8111	-2.81128
O4	***x***	-2.3476	-0.75978	0.19985
	y	-0.84091	-2.94359	-0.8145
	z	0.01052	-0.81165	-2.81025
O5	***x***	-2.34869	0.75865	0.19839
	y	0.83928	-2.9426	0.81367
	z	0.0094	0.8111	-2.81128
O6	***x***	-2.3476	0.75978	-0.19985
	y	0.84091	-2.94359	-0.8145
	z	-0.01052	-0.81165	-2.81025
O7	***x***	-2.34869	0.75865	-0.19839
	y	0.83928	-2.9426	-0.81367
	z	-0.0094	-0.8111	-2.81128
O8	***x***	-2.3476	0.75978	0.19985
	y	0.84091	-2.94359	0.8145
	z	0.01052	0.81165	-2.81025
Hf1	***x***	4.69629	0.00146	0.00155
	y	-0.00004	5.88619	0.25652
	z	0.00062	0.26763	5.62153
Hf2	***x***	4.69629	0.00146	-0.00155
	y	-0.00004	5.88619	-0.25652
	z	-0.00062	-0.26763	5.62153
Hf3	***x***	4.69629	-0.00146	0.00155

	y	0.00004	5.88619	-0.25652
	z	0.00062	-0.26763	5.62153
Hf4	***x***	4.69629	-0.00146	-0.00155
	y	0.00004	5.88619	0.25652
	z	-0.00062	0.26763	5.62153

Table S11. $Pca2_1$ of HfO_2 (a = 5.234 Å, b = 5.210 Å, c = 5.043 Å, P_r ~ 47.93 μC/cm^2)

Element	**Born Effective Charges**			
		x	***y***	***z***
O1	***x***	-2.34759	-0.79536	0.23357
	y	-0.89811	-2.99327	-0.80672
	z	0.01469	-0.80212	-2.79922
O2	***x***	-2.34793	-0.79437	-0.23216
	y	-0.89661	-2.99218	0.80623
	z	-0.01358	0.80173	-2.7992
O3	***x***	-2.34759	-0.79536	-0.23357
	y	-0.89811	-2.99327	0.80672
	z	-0.01469	0.80212	-2.79922
O4	***x***	-2.34793	-0.79437	0.23216
	y	-0.89661	-2.99218	-0.80623
	z	0.01358	-0.80173	-2.7992
O5	***x***	-2.34759	0.79536	0.23357
	y	0.89811	-2.99327	0.80672
	z	0.01469	0.80212	-2.79922
O6	***x***	-2.34793	0.79437	-0.23216
	y	0.89661	-2.99218	-0.80623
	z	-0.01358	-0.80173	-2.7992
O7	***x***	-2.34759	0.79536	-0.23357
	y	0.89811	-2.99327	-0.80672
	z	-0.01469	-0.80212	-2.79922
O8	***x***	-2.34793	0.79437	0.23216
	y	0.89661	-2.99218	0.80623
	z	0.01358	0.80173	-2.7992
Hf1	***x***	4.69553	-0.00149	-0.00181
	y	0.0001	5.98545	0.28112
	z	-0.0007	0.25179	5.59842
Hf2	***x***	4.69553	-0.00149	0.00181
	y	0.0001	5.98545	-0.28112
	z	0.0007	-0.25179	5.59842

Hf3	***x***	4.69553	0.00149	-0.00181
	y	-0.0001	5.98545	-0.28112
	z	-0.0007	-0.25179	5.59842
Hf4	***x***	4.69553	0.00149	0.00181
	y	-0.0001	5.98545	0.28112
	z	0.0007	0.25179	5.59842

Table S12. *P*ca2$_1$ of HfO_2 (a = 5.234 Å, b = 5.310 Å, c = 5.043 Å, P_r ~ 47.14 μC/cm^2)

Element	**Born Effective Charges**			
		x	***y***	***z***
O1	***x***	-2.35443	-0.82291	0.26826
	y	-0.94939	-3.02865	-0.79043
	z	0.01929	-0.7828	-2.79531
O2	***x***	-2.3497	-0.82339	-0.27205
	y	-0.95012	-3.03008	0.79067
	z	-0.02283	0.78326	-2.7945
O3	***x***	-2.35443	-0.82291	-0.26826
	y	-0.94939	-3.02865	0.79043
	z	-0.01929	0.7828	-2.79531
O4	***x***	-2.3497	-0.82339	0.27205
	y	-0.95012	-3.03008	-0.79067
	z	0.02283	-0.78326	-2.7945
O5	***x***	-2.35443	0.82291	0.26826
	y	0.94939	-3.02865	0.79043
	z	0.01929	0.7828	-2.79531
O6	***x***	-2.3497	0.82339	-0.27205
	y	0.95012	-3.03008	-0.79067
	z	-0.02283	-0.78326	-2.7945
O7	***x***	-2.35443	0.82291	-0.26826
	y	0.94939	-3.02865	-0.79043
	z	-0.01929	-0.7828	-2.79531
O8	***x***	-2.3497	0.82339	0.27205
	y	0.95012	-3.03008	0.79067
	z	0.02283	0.78326	-2.7945
Hf1	***x***	4.70413	0.00437	0.00524
	y	0.00085	6.05873	0.30483
	z	0.00152	0.23288	5.58981
Hf2	***x***	4.70413	0.00437	-0.00524
	y	0.00085	6.05873	-0.30483

	z	-0.00152	-0.23288	5.58981
Hf3	***x***	4.70413	-0.00437	0.00524
	y	-0.00085	6.05873	-0.30483
	z	0.00152	-0.23288	5.58981
Hf4	***x***	4.70413	-0.00437	-0.00524
	y	-0.00085	6.05873	0.30483
	z	-0.00152	0.23288	5.58981

Table S13. $P\mathrm{ca2_1}$ of HfO_2 (a = 5.234 Å, b = 5.410 Å, c = 5.043 Å, P_r ~ 46.60 μC/cm^2)

Element	**Born Effective Charges**			
		x	***y***	***z***
O1	***x***	-2.35779	-0.83804	0.31262
	y	-0.99162	-3.04803	-0.76701
	z	0.03273	-0.75563	-2.79922
O2	***x***	-2.36151	-0.84028	-0.3107
	y	-0.9941	-3.04682	0.7618
	z	-0.03086	0.75054	-2.79464
O3	***x***	-2.35779	-0.83804	-0.31262
	y	-0.99162	-3.04803	0.76701
	z	-0.03273	0.75563	-2.79922
O4	***x***	-2.36151	-0.84028	0.3107
	y	-0.9941	-3.04682	-0.7618
	z	0.03086	-0.75054	-2.79464
O5	***x***	-2.35779	0.83804	0.31262
	y	0.99162	-3.04803	0.76701
	z	0.03273	0.75563	-2.79922
O6	***x***	-2.36151	0.84028	-0.3107
	y	0.9941	-3.04682	-0.7618
	z	-0.03086	-0.75054	-2.79464
O7	***x***	-2.35779	0.83804	-0.31262
	y	0.99162	-3.04803	-0.76701
	z	-0.03273	-0.75563	-2.79922
O8	***x***	-2.36151	0.84028	0.3107
	y	0.9941	-3.04682	0.7618
	z	0.03086	0.75054	-2.79464
Hf1	***x***	4.7193	-0.00018	-0.00026
	y	0.0001	6.09485	0.32346
	z	0.00053	0.21582	5.59386
Hf2	***x***	4.7193	-0.00018	0.00026

	y	0.0001	6.09485	-0.32346
	z	-0.00053	-0.21582	5.59386
Hf3	***x***	4.7193	0.00018	-0.00026
	y	-0.0001	6.09485	-0.32346
	z	0.00053	-0.21582	5.59386
Hf4	***x***	4.7193	0.00018	0.00026
	y	-0.0001	6.09485	0.32346
	z	-0.00053	0.21582	5.59386

Table S14. *P*ca2$_1$ of HfO_2 (*a* = 5.234 Å, *b* = 5.510 Å, *c* = 5.043 Å, P_r ~ 47.14 μC/cm^2)

Element	**Born Effective Charges**			
		x	***y***	***z***
O1	***x***	-2.37511	-0.85604	0.36303
	y	-1.0407	-3.03649	-0.72122
	z	0.04624	-0.70323	-2.8091
O2	***x***	-2.37419	-0.85573	-0.36746
	y	-1.03712	-3.03619	0.71776
	z	-0.05014	0.70181	-2.81131
O3	***x***	-2.37511	-0.85604	-0.36303
	y	-1.0407	-3.03649	0.72122
	z	-0.04624	0.70323	-2.8091
O4	***x***	-2.37419	-0.85573	0.36746
	y	-1.03712	-3.03619	-0.71776
	z	0.05014	-0.70181	-2.81131
O5	***x***	-2.37511	0.85604	0.36303
	y	1.0407	-3.03649	0.72122
	z	0.04624	0.70323	-2.8091
O6	***x***	-2.37419	0.85573	-0.36746
	y	1.03712	-3.03619	-0.71776
	z	-0.05014	-0.70181	-2.81131
O7	***x***	-2.37511	0.85604	-0.36303
	y	1.0407	-3.03649	-0.72122
	z	-0.04624	-0.70323	-2.8091
O8	***x***	-2.37419	0.85573	0.36746
	y	1.03712	-3.03619	0.71776
	z	0.05014	0.70181	-2.81131
Hf1	***x***	4.7493	0.00232	0.00298
	y	0.00431	6.07267	0.34095
	z	0.00041	0.21164	5.62042

Hf2	***x***	4.7493	0.00232	-0.00298
	y	0.00431	6.07267	-0.34095
	z	-0.00041	-0.21164	5.62042
Hf3	***x***	4.7493	-0.00232	0.00298
	y	-0.00431	6.07267	-0.34095
	z	0.00041	-0.21164	5.62042
Hf4	***x***	4.7493	-0.00232	-0.00298
	y	-0.00431	6.07267	0.34095
	z	-0.00041	0.21164	5.62042

Table S15. *P*ca2$_1$ of HfO_2 (*a* = 5.234 Å, *b* = 5.610 Å, *c* = 5.043 Å, P_r ~ 45.58 μC/cm^2)

Element	**Born Effective Charges**			
		x	***y***	***z***
O1	***x***	-2.38186	-0.86693	0.4262
	y	-1.07334	-2.99538	-0.66141
	z	0.06948	-0.63653	-2.83173
O2	***x***	-2.38185	-0.8669	-0.42547
	y	-1.07368	-2.99532	0.66195
	z	-0.06876	0.63703	-2.83115
O3	***x***	-2.38186	-0.86693	-0.4262
	y	-1.07334	-2.99538	0.66141
	z	-0.06948	0.63653	-2.83173
O4	***x***	-2.38185	-0.8669	0.42547
	y	-1.07368	-2.99532	-0.66195
	z	0.06876	-0.63703	-2.83115
O5	***x***	-2.38186	0.86693	0.4262
	y	1.07334	-2.99538	0.66141
	z	0.06948	0.63653	-2.83173
O6	***x***	-2.38185	0.8669	-0.42547
	y	1.07368	-2.99532	-0.66195
	z	-0.06876	-0.63703	-2.83115
O7	***x***	-2.38186	0.86693	-0.4262
	y	1.07334	-2.99538	-0.66141
	z	-0.06948	-0.63653	-2.83173
O8	***x***	-2.38185	0.8669	0.42547
	y	1.07368	-2.99532	0.66195
	z	0.06876	0.63703	-2.83115
Hf1	***x***	4.76372	-0.00012	-0.00016
	y	-0.00048	5.9907	0.3517

	z	0.00001	0.22022	5.66287
Hf2	***x***	4.76372	-0.00012	0.00016
	y	-0.00048	5.9907	-0.3517
	z	-0.00001	-0.22022	5.66287
Hf3	***x***	4.76372	0.00012	-0.00016
	y	0.00048	5.9907	-0.3517
	z	0.00001	-0.22022	5.66287
Hf4	***x***	4.76372	0.00012	0.00016
	y	0.00048	5.9907	0.3517
	z	-0.00001	0.22022	5.66287

Table S16. *P*ca2$_1$ of HfO_2 (a = 5.2106 Å, b = 5.0074 Å, c = 5.276Å, P_r ~ 60.76 μC/cm^2)

Element	**Born Effective Charges**			
		x	***y***	***z***
O1	***x***	-2.41491	-0.87936	0.2009
	y	-0.96718	-2.86333	-0.78509
	z	0.00093	-0.77977	-2.94586
O2	***x***	-2.41533	-0.87965	-0.20075
	y	-0.96749	-2.86296	0.78508
	z	-0.00069	0.77972	-2.94508
O3	***x***	-2.41491	-0.87936	-0.2009
	y	-0.96718	-2.86333	0.78509
	z	-0.00093	0.77977	-2.94586
O4	***x***	-2.41533	-0.87965	0.20075
	y	-0.96749	-2.86296	-0.78508
	z	0.00069	-0.77972	-2.94508
O5	***x***	-2.41491	0.87936	0.2009
	y	0.96718	-2.86333	0.78509
	z	0.00093	0.77977	-2.94586
O6	***x***	-2.41533	0.87965	-0.20075
	y	0.96749	-2.86296	-0.78508
	z	-0.00069	-0.77972	-2.94508
O7	***x***	-2.41491	0.87936	-0.2009
	y	0.96718	-2.86333	-0.78509
	z	-0.00093	-0.77977	-2.94586
O8	***x***	-2.41533	0.87965	0.20075
	y	0.96749	-2.86296	0.78508
	z	0.00069	0.77972	-2.94508

Hf1	***x***	4.83024	0.00001	0.00005
	y	-0.00015	5.72629	0.29802
	z	0.00011	0.45391	5.89094
Hf2	***x***	4.83024	0.00001	-0.00005
	y	-0.00015	5.72629	-0.29802
	z	-0.00011	-0.45391	5.89094
Hf3	***x***	4.83024	-0.00001	0.00005
	y	0.00015	5.72629	-0.29802
	z	0.00011	-0.45391	5.89094
Hf4	***x***	4.83024	-0.00001	-0.00005
	y	0.00015	5.72629	0.29802
	z	-0.00011	0.45391	5.89094

References

[1] K. Liu, B. Dang, Z. Yang, T. Zhang, Z. Yang, J. Bai, Z. Pan. R. Huang, Y. Yang, Tuning the ferroelectricity of $Hf_{0.5}Zr_{0.5}O_2$ with alloy electrodes, Sci. China Inf. Sci. doi: 10.1007/s11432-023-3932-2.

[2] R. Cao, Y. Wang, S. Zhao, Y. Yang, X. Zhao, W. Wang, X. Zhang, H. Lv, Q. Liu, M. Liu, Effects of capping electrode on ferroelectric properties of $Hf_{0.5}Zr_{0.5}O_2$ thin films, IEEE Electron. Device Lett. 2018, 39 (8), 1207-1210.

[3] P. Xu, S. Yan, Y. Zhu, J. Zang, P. Luo, G. Li, Q. Yang, Z. Chen, W. Zhang, X. Zheng, M. Tang, Effects of different metal electrodes on the ferroelectric properties of HZO thin films, J. Mater. Sci: Mater. Electron. 2023, 34 (28), 1915.

[4] T. Shiraishi, S. Choi, T. Kiguchi, T. Shimizu, H. Funakubo, T. J. Konno, Formation of the orthorhombic phase in CeO_2-HfO_2 solid solution epitaxial thin films and their ferroelectric properties, Appl, Phys, Lett. 2019, **114** (23), 232902.

[5] S. Zheng, Z. Zhao, Z. Liu, B Zeng, L. Yin, Q. Peng, M. Liao, Y. Zhou, Improvement of remanent polarization of CeO_2-HfO_2 solid solution thin films on Si substrates by chemical solution deposition, Appl, Phys, Lett. 2020, **117** (21), 212904.

[6] Y. Tian, Y. Zhou, M. Zhao, Y. Ouyang, X. Tao, Effect of Ce doping on ferroelectric HfO_2 from first-principles: Implications for ferroelectric thin films and phase regulation, Sol. Stat. Chem. 2023,

328, 124316.

[7] S. S. Cheema, D. Kwon, N. Shanker, R. dos Reis, S.-L. Hsu, J. Xiao, H. Zhang, R. Wagner, A. Datar, M. R. McCarter, C. R. Serrao, A. K. Yadav, G. Karbasian, C.-H. Hsu, A. J. Tan, L.-C. Wang, V. Thakare, X. Zhang, A. Mehta, E. Karapetrova, R. V. Chopdekar, P. Shafer, E. Arenholz, C. Hu, R. Proksch, R. Ramesh, J. Ciston, S. Salahuddin, Enhanced ferroelectricity in ultrathin films grown directly on silicon, Nature, 2020, **580** (7804), 478-482.

[8] C. Lee,1 E. Cho, H, Lee, C. Hwang, S. Han, First-principles study on doping and phase stability of HfO_2, Phys. Rev. B, 2008, 78, 012102.

[9] S. M. Park, S. G. Lee, S. E. Yun, Ferroelectric properties of Pb (Zr, Ti)O_3 films fabricated using a modified sol-gel based process, Thin Solid Films, 2008, 516, 5282-5286.

[10] M. Antik, K. L. Megan, E. B. Thomas, F. I. Jon, S. Nikhil, Oxygen vacancy contributions to the electrical stress response and endurance of ferroelectric hafnium zirconium oxide thin films, Appl, Phys, Lett. 2023, 122 (13), 132902.